Ratiometric Fluorescent Polymeric Thermometer for Thermogenesis Investigation in Living Cells

ARTICLE *in* ANALYTICAL CHEMISTRY · SEPTEMBER 2015

Impact Factor: 5.64 · DOI: 10.1021/acs.analchem.5b02791

analytical chemistry

Article

pubs.acs.org/ac

Ratiometric Fluorescent Polymeric Thermometer for Thermogenesis Investigation in Living Cells

Juan Qiao,[†,⊥] Yoon-Ho Hwang,[‡,⊥] Chuan-Fang Chen,[§] Li Qi,[*,†] Ping Dong,[∥] Xiao-Yu Mu,[†] and Dong-Pyo Kim[*,‡]

[†]Beijing National Laboratory for Molecular Sciences, Key Laboratory of Analytical Chemistry for Living Biosystems, Institute of Chemistry, Chinese Academy of Sciences, No. 2 Zhongguancun Beiyijie, Beijing 100190, People's Republic of China

[‡]National Creative Research Center of Applied Microfluidic Chemistry, Department of Chemical Engineering, Pohang University of Science and Technology, Pohang, Gyeongbuk 790-784, Republic of Korea

[§]Beijing Key Laboratory of Bioelectromagnetism, Institute of Electrical Engineering, Beijing, 100190, People's Republic of China

[∥]Research Centre of Plastic Surgery Hospital, Chinese Academy of Medical Sciences and Peking Union Medical College, Beijing, 100730, People's Republic of China

Supporting Information

ABSTRACT: Intracellular temperature has a fundamental effect on cellular events. Herein, a novel fluorescent polymer ratiometric nanothermometer has been developed based on transferrin protein-stabilized gold nanoclusters as the targeting and fluorescent ratiometric unit and the thermosensitve polymer as the temperature sensing unit. The resultant nanothermometer could feature a high and spontaneous uptake into the HeLa cells and the ratiometric temperature sensing over the physiological temperature range. Moreover, the precise temperature sensing for intracellular heat generation in HeLa cells following calcium ions stress has been achieved. This practical intracellular thermometry could eliminate the interference of the intracellular surrounding environment in cancer cells without a microinjection procedure, which is user-friendly. The prepared new nanothermometer can provide tools for unveiling the intrinsic relationship between the intracellular temperature and ion channel function.

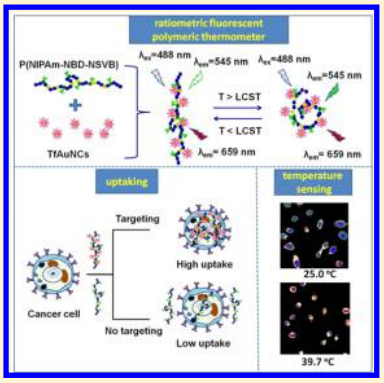

Temperature is a fundamental physical quantity that governs the cellular events inside complex intracellular circumstances, which keep tight relationship with the cell structure and function, including cell division, gene expression, enzyme reaction, and metabolism.[1] In detail, the transmembrane transport of ions,[2] the signal transduction,[3] energy conversion,[4] and cell division[5] would be greatly influenced by the fluctuation of intracellular temperature. For instance, in the fundamental ATP hydrolysis processes, obvious thermogenesis has been observed and the intracellular thermometer also can monitor the hydrolysis rate, underlying the present bioenergetics.[6] Moreover, superfluous energy was released in the form of heat during the ATP production in the mitochondria.[7] Furthermore, some of the ion pumps changing, such as calcium ions shock, would boost heat production and tune the intracellular temperature by promoting the activities of the ion pumps and speed up the respiration rates.[8] Interesting, the ion channel on the cell membranes formed by temperature-sensitive vanilloid receptor-like proteins, such as TRPV1[2] and TRPV3,[9] will open and cause the influx of calcium ions with the local temperature increasing. Thus, determination and monitoring intracellular temperature will greatly contribute to the deep understanding of intricate cell biological processes.

Recently, several works have been proposed to address the requirement for measuring intracellular temperature,[10−12] such as quantum dots,[8,13] polymers,[6,14−16] biomacromolecules,[17−19] and gold nanoclusters,[20] which rely on injection or uptake of nano-objects into living cells. Compared to conventional nanothermometers, the fluorescent polymeric thermometers,[15] which are composed of a fluorescent molecule and polymer, are promising tools for intracellular temperature sensing and mapping, owing to their function at the molecular level. Nevertheless, when considering setup tools for intracellular temperature sensing using the fluorescent polymeric thermometer, the researchers still have suffered some limitations. For example, most of the fluorescent polymeric thermometers for intracellular thermometry require a microinjection technique for introducing them into living cells, which might injure the living cells and disturb the cells' activity. Thus, it is clear that, except for the high temperature resolution and high spatial resolution requirement, the ideal fluorescent polymeric thermometer should possess multiple properties which could reach the demands including introducing the thermometer into the cells without causing the cells' activity to be disturbed and function independence of the surrounding environmental pH, ionic strength, and biomacromolecules.[21,22]

Received: July 24, 2015
Accepted: September 22, 2015
Published: September 22, 2015

DOI: 10.1021/acs.analchem.5b02791
Anal. Chem. 2015, 87, 10535−10541

To resolve these limitations, some efforts have been attempted.[14,23] However, the thermoresponse sensitivity of the reported fluorescent polymeric thermometers decreased. Moreover, most of them described the intracellular temperature value only with a single wavelength, which could not avoid the effect of the surrounding environment. Thus, design and preparation of a new fluorescent polymeric thermometer simultaneously possessing the spontaneous target and ratiometric fluorescence features, which could satisfy the requirements for intracellular temperature sensing, are highly desirable and challenging.

Relying on the development of nanotechnology,[24] fluorescent gold nanoclusters (AuNCs), especially protein-protected AuNCs,[25] have emerged as by far one of the most promising classes of tools for biosensing, in vitro and in vivo imaging, and also in cancer therapy. Therefore, a strategy to propose an ideal intracellular thermometer based on AuNCs was put forward in the present study. First, the fluorescent polymeric thermometer composed of fluorescent dyes and thermosensitive polymer was selected as the temperature sensing part for intracellular temperature sensing and imaging. Second, transferrin protein-stabilized AuNCs (TfAuNCs), which could easily target the cancer cells and accelerate the spontaneous uptake process, were chosen as the cancer cells targeting part and the ratiometric fluorescent part. In addition, to bond the thermosensitive part and the ratiometric part, a novel linkage monomer was copolymerized in the fluorescent polymeric thermometer framework. On the basis of this design proposal, the nanoconjugate was synthesized and characterized. Moreover, the complete experiment and analysis for the intracellular temperature ratiometric fluorescent sensing and imaging were presented in detail. For the application of the nanothermometer, the investigation of the time-related response of localized intracellular temperature for prolonged periods after chemical calcium ion shock by chemical inducement was carried out, reporting the experimental evidence.

EXPERIMENTAL SECTION

Chemicals and Materials. *N*-Hydroxysuccinimide (NHS), 4-vinylbenzoic acid, *N*-isopropylacrylamide (NIPAm), *N*,*N*′-dicyclohexylcarbodiimide (DCC), 4-dimethylaminopyridine (DMAP), and 2,2′-azobis(2-methylpropionitrile) (AIBN) were purchased from Aladdin Reagents Industrial Co., Ltd. (Shanghai, China). $NaHCO_3$, $MgSO_4$, ethyl ether, and 1,4-dioxane were obtained from Beijing Chemical Works (Beijing, China). The transferring from bovine plasma was obtained from Shenyang Bioing Biotechnology Co., Ltd. (Shenyang, China). Chloroauric acid ($HAuCl_4{\cdot}3H_2O$) was bought from Shenyang Jinke Reagent Factory (Shenyang, China). We purchased the commercially available CCK-8 kit from Beijing Tianenze Corporation (Beijing, China). All other chemicals were purchased from Aladdin Reagents Industrial Co., Ltd. (Shanghai, China) and used without further purification. Ultrapure water (18.2 MΩ) was used throughout the experiments. The chain transfer agent (CTA) *S*,*S*′-bis(α,α′-dimethylacetic acid) trithiocarbonate (DATB) was synthesized according to ref 26. (4-(2-acryloylaminoethylamino)-7-nitro-2,1,3-benzoxadiazole) (NBDAA) was synthesized in our lab, and the detail process was reported in ref 22.

The solutions for the cell culture, such as phosphate-buffered saline (PBS) solution, Dulbecco's modified Eagle's medium (DMEM), and 0.25% trypsin, were purchased from Hyclone Laboratories Inc. (Utah, U.S.A.). The fetal bovine serum, penicillin (100 μg/mL), and streptomycin (100 μg/mL) were obtained from Gibco Life Technologies Corporation (U.S.A.). The ionomycin (calcium salt) was from Cayman Chemical Company (Michigan, U.S.A.).

Synthesis of *N*-Succinimide *p*-Vinylbenzoate (NSVB). As shown in Figure S1 in the Supporting Information, NHS (1.2 g, 10.1 mmol) and 4-vinylbenzoic acid (1.0 g, 6.7 mmol) were mixed with ethyl acetate (25 mL) and stirred until all solids dissolved. DCC (2.1 g, 10.1 mmol) and DMAP (41.2 mg, 0.53 mmol) were added, and the solution stirred at room temperature for 36 h at which time a white precipitate was formed. The solution was filtered and then concentrated by rotary evaporation to give a yellow oily residue that was dissolved in DCM, extracted with saturated aqueous $NaHCO_3$ solution (3 × 20 mL), washed with water (3 × 20 mL), dried over $MgSO_4$, and concentrated to an oil. This oil was redissolved in DCM (30 mL) and ethyl ether (170 mL) to give a white solid (0.63 g, 60% yield). The structure of the NSVB was confirmed by the ^{1}H NMR in Figure S2 in the Supporting Information.

Synthesis of P(NIPAm−NBD−NSVB). NIPAm (0.6 g), NSVB (12.0 mg), NBDAA (13.8 mg), CTA (DATB, 14.0 mg), and AIBN (0.8 mg) were mixed with 1,4-dioxane (5 mL). The mixture was degassed by three freeze−pump−thaw cycles, sealed under nitrogen, and heated at 70 °C under nitrogen for 24 h (Figure S3 in the Supporting Information). After cooling, the mixture was dissolved in 1,4-dioxane (5 mL) and precipitated twice in ethyl ether (100 mL). The light pink solid was dried under vacuum to give the desired P(NIPAm−NBD−NSVB) (485 mg, 75% conversion).

The polymer P(NIPAm−NBD−NSVB) was prepared in a droplet-based microfluidic reactor which composed by a T-junction and a tube as shown in Figure S4 in the Supporting Information. The polymerization solution containing NIPAm (0.6 g), NSVB (12.0 mg), NBDAA (13.8 mg), CTA (DATB, 14.0 mg), AIBN (0.8 mg), and 5.0 mL 1,4-dioxane was degassed by a freeze−pump−thaw method. Then the polymerization solution drawn into a syringe and pumped into the T-junction to form droplets. The tube was heated to 80 °C until the reaction was complete and then cooled to room temperature. The products were then collected and purified as the above procedure. Different polymerization reaction times depending on the flow rates were studied in detail (Table S1 in the Supporting Information). The structure of the NSVB was determined by the ^{1}H NMR in Figure S5 in the Supporting Information.

Synthesis of TfAuNCs. The TfAuNCs were synthesized by a simple, one-pot, and "green" route at the mild conditions.[27] Briefly, aqueous solution of Tf (4.0 mL, 10.0 mg mL^{-1}) and aqueous solution of the $HAuCl_4$ (2.0 mL, 5.0 mM) were mixed together under vigorous stirring at 37 °C.[27] Then, 20.0 μL of ascorbic acid (0.35 mg mL^{-1}) was added into the mixture solution dropwise. The NaOH solution (0.2 mL, 1.0 M) was introduced into the mixture solution after 5 min, and the reaction was preceded in the 37 °C oil bath for 3 h. According to ref 27, the optimal molar ratio of Au/Tf was 1:20 for formation of TfAuNCs. The role of the ascorbic acid was to trigger the formation of AuNCs under a low concentration of Tf. During the reaction, the color of the solution changed from colorless to pale brown. After 3 h of reaction, the solution was ultrafiltrated of the TfAuNCs with the viva spin column and ultrafiltration membrane (Sartorius AG, Gottingen, Germany/3000 Da) at 10 000 run min^{-1} for 10 min and kept in 4 °C for

DOI: 10.1021/acs.analchem.5b02791
Anal. Chem. 2015, 87, 10535−10541

further use (Figure S6 in the Supporting Information). The excess NaOH and the residual Tf proteins, which did not react with the AuNCs, were removed.

Synthesis of P(NIPAm−NBD−NSVB)−TfAuNCs. P(NIPAm−NBD−NSVB) polymer (5.0 mg) was dissolved in 1.0 mL of different concentration of TfAuNCs solutions, then the NSVB group in the polymer reacted with amino groups in the Tf proteins at room temperature for 3 h with stirring. The reactant solution was ultrafiltrated by the membrane (Sartorius AG, Gottingen, Germany/3000 Da) at 10 000 run min^{-1} for 10 min to remove the excess polymer.

RESULTS AND DISCUSSION

To synthesize the thermosensitive polymers and combine with the AuNCs, the linkage monomer NSVB was prepared first (Figures S1 and S2 in the Supporting Information).[28] Figure S3 displays the synthesis reaction of the thermosensitive polymer. The feed ratio of the NIPAm/NBDAA/NSVB was 100:1:1 for the synthesis of the P(NIPAm−NBD−NSVB) because that higher ratio of NBDAA and NSVB would influence the fluorescent temperature sensing sensitivity and the solubility of the polymer.[6,15] Then the fluorescent dyes (NBDAA), the thermosensitive polymer, and the linkage monomer NSVB were polymerized using the reversible addition−fragmentation chain transfer (RAFT) method with a droplet-based microfluidic reactor (Figure S4, Supporting Information). According to our previous work,[29] it has been observed that, compared with the polymer synthesized in conventional flask reactor, the fluorescent thermosensitive polymer synthesized in the droplet-based microfluidic reactor could possess lower polymer distribution index (PDI) within short polymerization process due to its advantages[30,31] such as effective mass transfer and heat transfer, better mixing,[32] and precise reaction time control (Table S1, Supporting Information). Finally, the prepared P(NIPAm−NBD−NSVB) with the molecular weight of 5.9 kDa and PDI 1.21 was selected for further study due to more active groups and the better PDI results. The actual compositions of the synthesized thermosensitive polymers were determined by ^{1}H NMR as shown in Figure S5.

The excitation and emission spectra of the TfAuNCs solutions were investigated, and the results are illustrated in Figure 1. The TfAuNCs solutions emitted strong red emission at 659 nm, and the quantum yield of the TfAuNCs was 1.8% (fluorescein used as reference). The diameter of the synthesized TfAuNCs has been detected to be 5.6 ± 1.0 nm, which is in agreement with the reported results.[27]

The NSVB represents a novel activated ester monomer that readily reacted with amino groups which can be covalently linked to the surface of the TfAuNCs. Thus, as exhibited in Figure 2, the polymer that contained NSVB as a more active

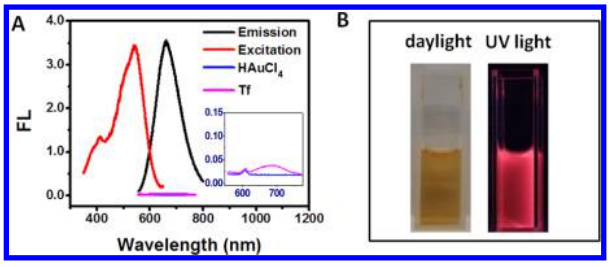

Figure 1. (A) Excitation and emission spectra of Tf, $HAuCl_4$, and TfAuNCs at room temperature. Inset: magnified spectra of Tf and $HAuCl_4$. (B) The photographs of TfAuNCs solution under daylight and long-wavelength UV lamp with excitation at 365 nm.

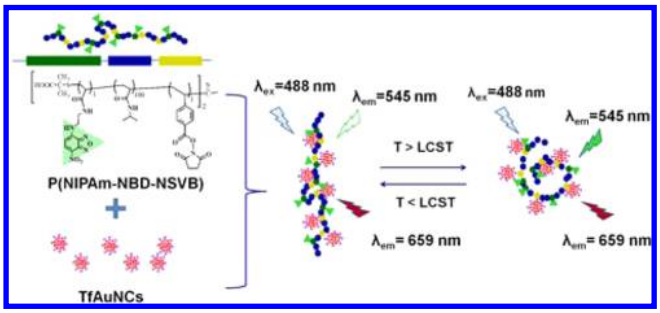

Figure 2. Schematic diagram of the synthetic route for P(NIPAm−NBD−NSVB)−TfAuNCs and its ratiometric thermosensitive property.

moiety toward amino groups of Tf protein was reacted with the TfAuNCs, and finally the polymer−TfAuNCs was obtained. Interestingly, NBDAA is a solvent polarity-responsive dye,[33] and our results exhibited that its fluorescent intensity was much higher in nonpolar solvent ($CHCl_3$) than that in aqueous solution (Figure S7 in the Supporting Information). Furthermore, as described in refs 14−16, 22, and 33, the fluorescent intensity of NBDAA would change obviously with the temperature increasing when NBDAA was copolymerized with PNIPAm. It can be explained by the properties of NBDAA and PNIPAm. On the one hand, it has been reported that the fluorescent intensity of NBDAA would increase when the polarity of the surrounding condition was altered from hydrophilicity to hydrophobicity.[6,15,22] On the other hand, when the temperature increased above the lower critical solution temperature (LCST) of PNIPAm, the intermolecular hydrogen bond formed by PNIPAm and water molecule no longer existed, leading to the surrounding condition changing from hydrophilicity to hydrophobicity. Thus, when NBDAA was copolymerized in PNIPAm chains, the fluorescent intensity of the prepared P(NIPAm−NBD−NSVB) would increase with temperature increasing. Further, the TfAuNCs were introduced as the targeting and fluorescent ratiometric unit to enhance its ability of entrance into the cells. Moreover, the ratiometric property of the TfAuNCs could let us obtain more robust signals and can eliminate most of the ambiguities in cells. However, the experimental results showed that the amount of the TfAuNCs reacted with the polymer would influence the thermosensitive property of the nanoconjugates. Different concentrations of TfAuNCs (1.3, 1.1, 0.8, and 0.5 mM) were reacted with the polymer (5.0 mg mL^{-1}). Then, the spectra of the fluorescent intensity changing with the temperature and the R (calculated from I_{545}/I_{659}) versus concentration of TfAuNCs at different temperatures have been investigated (Figure S8 in the Supporting Information). The results displayed that only 0.8 mM TfAuNCs reacting with the polymer could create the best thermosensitive property; thus, the concentration ratio of polymer to TfAuNCs (5.0 mg mL^{-1}; 0.8 mM) was finally chosen for further study. The dynamic light scattering (DLS) detection results revealed that the diameters of polymer, TfAuNCs and the obtained polymer−TfAuNCs were 3.0 ± 0.2 nm, 5.6 ± 1.0 and 68.1 ± 3.2 nm (Figure S9 in the Supporting Information), respectively.

To evaluate the application of the thermosensitive polymer−TfAuNCs for the intracellular temperature sensing, the LCST

DOI: 10.1021/acs.analchem.5b02791
Anal. Chem. 2015, 87, 10535−10541

of the synthesized polymer−TfAuNCs was investigated by using a turbidity method (Figure 3A), which contained the

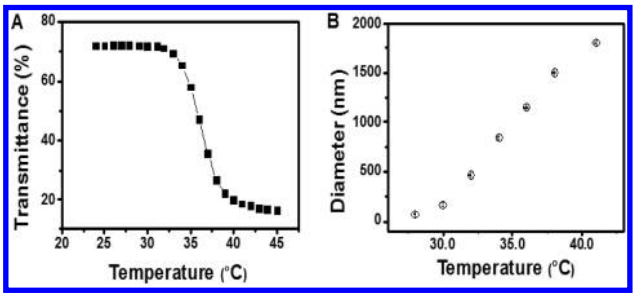

Figure 3. Characterization of the polymer−TfAuNCs. (A) Transmittance changes of the polymer−TfAuNCs aqueous solutions as a function of temperature. (B) The diameter change of the polymer−TfAuNCs with temperature variation.

TfAuNCs and a linkage monomer polymerized in the framework. The LCST of the polymer−TfAuNCs determined in this work is 35.5 °C, which temperature conversion range is suitable for intracellular temperature sensing and is comparable with ref 34. Moreover, the DLS method has been used for the investigation of the diameter changes of the polymer−TfAuNCs with temperature variation. The results displayed that the diameters of the polymer−TfAuNCs at lower temperature (70.9 ± 6.8 nm) increased to be 1805.0 ± 11.8 nm with the temperature changing from 28 to 41 °C (Figure 3B).

To confirm the feasibility of the polymer−TfAuNCs for intracellular nanothermometry, we carefully studied the thermosensitive property of the nanoconjugates. The single excitation wavelength (488 nm) was chosen to adapt the excitation demands of the polymer and the TfAuNCs, which can avoid the disadvantage of dual excitation mode including measurement fluorescence intensities at two excitation wavelengths and provide a built-in correction for environmental effects. The fluorescent emission spectrum of the polymer−TfAuNCs at different temperatures was investigated, and the results are displayed in Figure 4A. The magnified fluorescence spectra of Figure 4A for the changing of the ratiometric signal of TfAuNCs with the temperature increasing are displayed in Figure S10 in the Supporting Information. The data reveal that the fluorescent intensity of NBDAA in the polymer at 545 nm increased obviously with the temperature, while the fluorescent intensity of TfAuNCs at 659 nm also changed rather than be invariable. It is speculated that the fluorescent intensity increasing of TfAuNCs at 659 nm might own to the overlap of the spectra, which caused the slight increasing with the temperature. This phenomenon would not interfere in the ratio measurement because the temperature sensing results were obtained from the intensity ratio of the NBDAA in the polymer at 545 nm and TfAuNCs at 659 nm (I_{545}/I_{659}). The average fluorescent intensity ratio (I_{545}/I_{659}) of the polymer−TfAuNCs changed close to linearly with temperature; the fit yielded a correlation coefficient of 0.985 (Figure 4B). Therefore, the fluorescent intensity ratio (I_{545}/I_{659}) increasing with the temperature and the reversibility of six cycles indicated the excellent cycling capability of the prepared polymer−TfAuNCs between 28 and 41 °C (Figure 4C). Moreover, under continuous excitation with the UV lamp for 40 min, the average fluorescent intensity ratio (I_{545}/I_{659}) of the polymer−TfAuNCs remained essentially constant (Figure 4D).

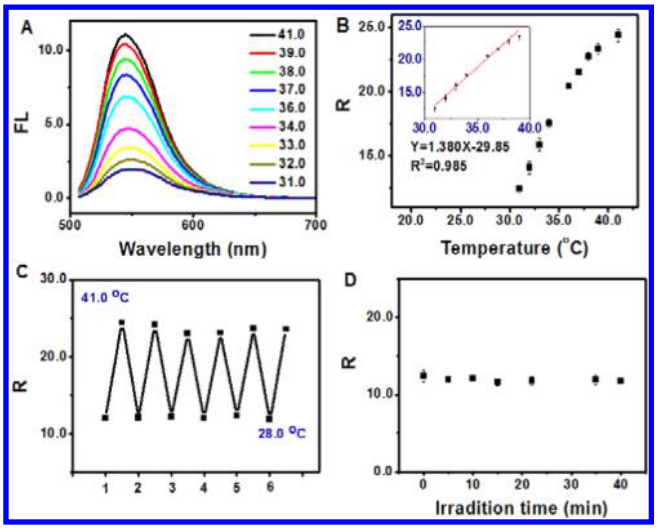

Figure 4. (A) Fluorescence spectra of the ratiometric temperature-responsive polymer−TfAuNCs at 488 nm excitation at different temperatures ranging from 31 to 41 °C. (B) Temperature-responsive calibration plot of the ratiometric polymer−TfAuNCs. Inset: temperature-responsive calibration curve of polymer−TfAuNCs. The data R were calculated from the ratio of the fluorescence intensities (I_{545}/I_{659}). The polymer−TfAuNCs were composed of P(NIPAm−NBD−NSVB)−TfAuNCs (5.0 mg mL^{-1}; 0.8 mM). (C) Fluorescence ratio of polymer−TfAuNCs upon cycling the temperature 5 times between 28 and 41 °C. (D) Fluorescence ratio of polymer−TfAuNCs as a function of irradiation time. The excitation intensity was kept constant using the UV lamp.

The thermoresponsive performance of the polymer−TfAuNCs in intracellular species such as electrolytes, pH, and proteins was assessed by a spectrofluorometer. Potassium chloride was chosen as the ion source to simulate the intracellular conditions due to the high concentration of potassium ion in the cytoplasm. The results demonstrated in Figure S11A in the Supporting Information indicated the fluorescent intensity of the polymer−TfAuNCs changed with the temperature at different potassium ion concentrations, which illuminated the negligible effect of the electrolytes. Then the fluorescence response of polymer−TfAuNCs to environmental pH (3.0−10.5) has been investigated (Figure S11B in the Supporting Information). It has been found that fluorescence response of polymer−TfAuNCs was almost independent of buffer pH, except at pH 3.0, 9.2, and 10.5. As in most cases, the intracellular physiological solution was at neutral pH; thus, the thermoresponsive performance of the polymer−TfAuNCs was less affected by the environmental pH in cell. Moreover, the performance of the polymer−TfAuNCs influenced by the surrounding protein in the solution, such as bovine serum albumin, was studied (Figure S11A in the Supporting Information). The response time of the polymer−TfAuNCs has been recorded at 39 °C, and the data is exhibited in Figure S11C. Our results revealed that the temperature response time of the polymer−TfAuNCs was 40 s. Therefore, the temperature response of the resultant polymer−TfAuNCs should be suitable for further investigation of temperature change in the cells. These results indicated that the obtained polymer−TfAuNCs have a high capability for accurate intracellular temperature sensing.

To assess the biocompatibility of the polymer−TfAuNCs, the cellular toxicity to the cells was studied using CCK-8 assay. The results (Figure S11D in the Supporting Information)

DOI: 10.1021/acs.analchem.5b02791
Anal. Chem. 2015, 87, 10535−10541

displayed minor slight difference in cell death over 12 h for the treated versus untreated cells. The concentrations of polymer−TfAuNCs ranging from 0.05 to 0.80 mg mL^{-1} were tested, and the results demonstrated that the polymer−TfAuNCs only induced a slight decrease (about 8% of control) in cell viability and exhibited good biocompatibility. Therefore, all of these results indicated that the polymer−TfAuNCs have no obvious cytotoxicity to the HeLa cells during a prolonged period of time.

The schematic for the polymer−TfAuNCs spontaneous uptake into the HeLa cells has been exhibited in Figure S12 in the Supporting Information. It is speculated that, after introducing the targeting part (TfAuNCs) into the thermosensitive polymer, much more polymer−TfAuNCs should be drawn in the HeLa cells and the ratiometric fluorescent sensing of the intracellular temperature would be completed. Thus, the performance of the polymer−TfAuNCs for the spontaneous uptake of the HeLa cells and the intracellular temperature sensing has been examined in detail. First, representative differential interference contrast (DIC) and confocal fluorescence images of HeLa cells treated with the fluorescent copolymers are shown in Figure S13 in the Supporting Information. The results displayed that the polymer−TfAuNCs could diffusely distribute within the cytoplasm, whereas the polymer−TfAuNCs were observed much more than the polymer in the fluorescence images of HeLa cells.

These results were also clearly proved by the flow cytometry method, which assisted the spontaneous uptake of the polymer−TfAuNCs into the HeLa cells (Figure S14 in the Supporting Information). When compared with the control HeLa cells (Figure S14A in the Supporting Information), the lower right quadrant of the polymer cytogram (Figure S14B in the Supporting Information) showed the cells were positive for polymer binding (22.2%). The upper right quadrant of the polymer−TfAuNCs cytogram (Figure S14C in the Supporting Information) showed the cells were positive for polymer−TfAuNCs binding (3.6%). Moreover, the cell amount in the lower right quadrant of the polymer−TfAuNCs cytogram (Figure S14C in the Supporting Information) increased from 22.2% to 88.0%. These experimental data revealed that more polymer−TfAuNCs could be introduced into the HeLa cells significantly. Meanwhile, the results were also exhibited in the flow cytometric quantification histograms of intracellular polymer and polymer−TfAuNCs in HeLa cells (Figure 5). Then the spontaneous uptake efficiencies of the polymer−TfAuNCs into the HeLa cells at 25 °C were investigated by the flow cytometry method taken at different incubation times ranging from 20 min to 3 h (Figure S15 in the Supporting Information). The florescent intensity of the cells incubated with the polymer−TfAuNCs increased with the incubation time. The data indicated that the polymer−TfAuNCs could be spontaneously introduced into the HeLa after treatment for only 20 min and the uptake efficiency of the polymer−TfAuNCs into HeLa cells increased as the incubation time increased. Finally, 3 h of incubation of the cells with the polymer−TfAuNCs solution has been chosen for further study.

To demonstrate the applicability of polymer−TfAuNCs for sensing of the intracellular temperature variation more directly and accurately, the detailed fluorescence imaging analysis was studied using the prepared polymer−TfAuNCs for the temperature sensing. The intracellular calibration experiment was investigated in HeLa cells first by the polymer−TfAuNCs, and the representative fluorescence imaging with temperature

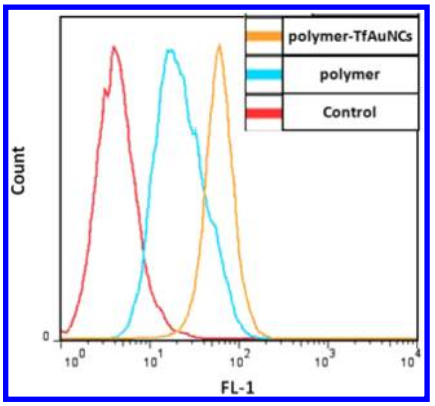

Figure 5. Flow cytometric quantification of intracellular polymer and polymer−TfAuNCs in HeLa cells (histograms). The polymer−TfAuNCs were composed of P(NIPAm−NBD−NSVB)−TfAuNCs (5.0 mg mL^{-1}; 0.8 mM).

increasing ranging from 25 to 39.7 °C is displayed in Figure 6A. The results also revealed that the polymer−TfAuNCs were dispersed in the cytoplasm without transferring to the nucleus. During the process of the experiment, the ratio imagings were

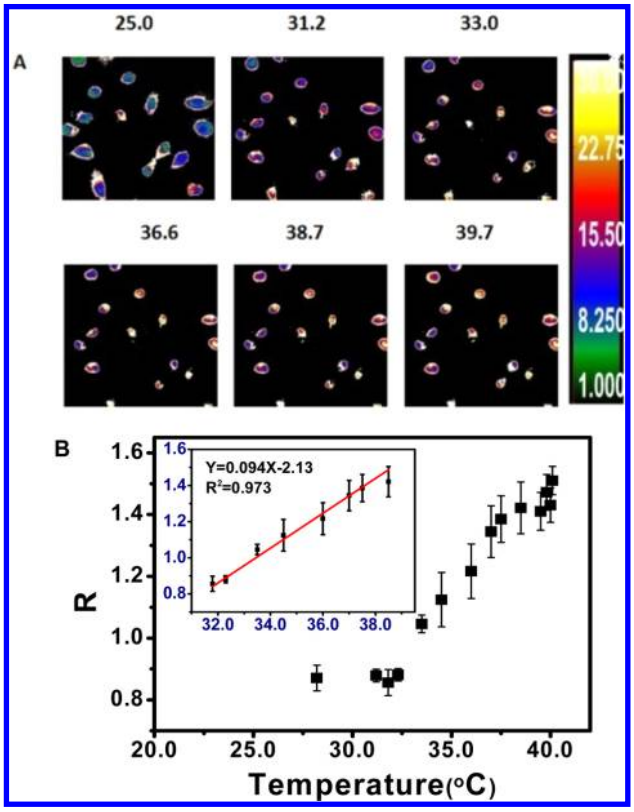

Figure 6. (A) Fluorescent images ratio channel generated by Olympus software (FV10-ASW) of HeLa cells at different temperatures of 25.0, 31.2, 33.0, 36.6, 38.7, and 39.7 °C, respectively. The images are ratiometric results of the GFP channel [P(NIPAm−NBD−NSVB)] and the CY3 channel (TfAuNCs) that were collected in the ranges of about 510−560 and 570−670 nm, respectively. The polymer−TfAuNCs were composed of P(NIPAm−NBD−NSVB)−TfAuNCs (5.0 mg mL^{-1}; 0.8 mM). (B) The intracellular fluorescent intensity ratios (R at the y-axis) obtained from the images changed with increasing temperature. Inset: intracellular temperature-responsive calibration curve of polymer−TfAuNCs obtained from five different cells in the fluorescence images.

DOI: 10.1021/acs.analchem.5b02791
Anal. Chem. 2015, 87, 10535−10541

obtained in the emission ranges of the GFP dye (about 510−560 nm) and the Cy3 dye (about 570−670 nm), and the photomicrogram instrument (Olympus ix83) was applied for generating of the ratio channel temperature sensing images. The imaging of the ratio channel, which was collected based on the GFP and Cy3 channels, indicated a characteristic temperature-dependent signal, and a good linear calibration curve was generated. The calibration curve for intracellular temperature sensing within the temperature range from 31.8 to 38.5 °C (Figure 6B, inset) was calculated based on the relationship between the whole cells fluorescence intensity ratio (GFP/CY3) in the images and temperature, which got the good linear calibration ($y = 0.094x - 2.13$) with a correlation coefficient of 0.973. On the basis of the imaging collecting instrument, the temperature resolution of the thermal response of polymer−TfAuNCs in the HeLa cells was about 0.3−0.5 °C, which could be comparable to other optical thermometers.[22]

For further illustrating the temperature sensing and imaging capability of polymer−TfAuNCs, a chemically induced thermogenesis method was developed to investigate subcellular temperature responses in single living cells on the basis of linear curve. Calcium ion shock was applied to boost intracellular heat production, possibly by accelerating the activities of ion pumps by the ionomycin calcium complex and promoting the respiration rates of the mitochondrion. For detail process, the polymer−TfAuNCs were incubated with the HeLa cells first, then calcium ion (10 nM) were incubated with the HeLa cells for 30 min before the ionomycin calcium complex solution (1 μM) was added. Finally, 2 min later, the time course of the relationship between the fluorescence intensity ratio (GFP/CY3) of five different single HeLa cells in the images and temperature were determined. After the calcium ion burst, the intracellular ratio calculated from the fluorescence ratio of polymer−TfAuNCs increased. This result strongly indicated the intracellular heat production at each of their specific locations. In the representative result displayed in Figure 7, the intracellular temperature was approximately 34.5 °C before ionomycin addition, and it rose to approximately 39 °C (cell 3) after ionomycin calcium complex solution treatment within 2 min. Then in the following several minutes, the temperature almost keep constant with a slightly decrease after 4 min, which preceded the shrinking of the cell. These results probably indicated the end stage of heat production originally induced by ionomycin and then the end of cellular activities due to cell death. These above calcium ions shock experiment results revealed that the intracellular events related to the temperature changing could be studied by the novel polymer−TfAuNCs as the nanothermometer.

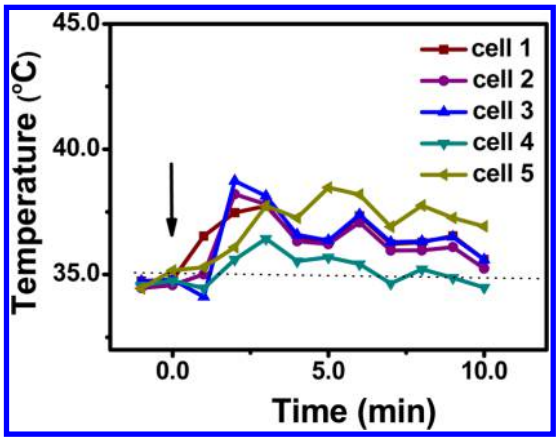

Figure 7. Intracellular temperature shifts as a function of time response to Ca^{2+} shock: the temperature measurement as estimated from the average fluorescent intensity of the cancer cells. The ratio was the obtained fluorescent intensities of the GFP channel [P(NIPAm−NBD−NSVB)] and the CY3 channel (TfAuNCs) that were collected in the ranges of about 510−560 and 570−670 nm, respectively. The temperature was calculated by the calibration plot in Figure 6.

It should be noted that the proposed polymer−TfAuNCs could sensitively probe living cell temperature variations by analyzing the average fluorescence changing with the temperature resolution of 0.3−0.5 °C in the range of 31.8−38.5 °C, which is well-compared with other fluorescent polymer-based thermosensitive materials (Table S2 in the Supporting Information).

CONCLUSIONS

In this work, a novel kind of fluorescent polymeric nanothermometer has been designed and synthesized in the study. This nanothermometer used TfAuNCs as the targeting part for the spontaneous uptake and fluorescent ratiometric part and used the thermosensitve polymer [P(NIPAm−NBD−NSVB)] as the temperature sensing part, which featured a high uptake into the HeLa cells and temperature sensitivity of their fluorescent ratio imaging over the physiological temperature range. The polymeric nanothermometer also enables precise temperature sensing in biological systems for intracellular heat generation in HeLa cells following calcium ions stress by the ionomycin inducement. On the basis of these unique advantages, this nanothermometer has the potential to become a powerful tool for unraveling intimate cellular processes that involve thermogenesis in the cell level.

ASSOCIATED CONTENT

Supporting Information

The Supporting Information is available free of charge on the ACS Publications website at DOI: 10.1021/acs.analchem.5b02791.

Experimental details, Figures S1−S15, and Tables S1 and S2 (PDF)

AUTHOR INFORMATION

Corresponding Authors

*E-mail: qili@iccas.ac.cn. Phone: +86-10-82627290.
*E-mail: dpkim@postech.ac.kr. Phone: +82-54-2792272.

Author Contributions

⊥J.Q. and Y.-H.H. contributed equally to this work.

Notes

The authors declare no competing financial interest.

ACKNOWLEDGMENTS

We gratefully acknowledge financial support from NSFC (Grants 21475137, 21375132, 21175138, 21205125, 21135006 and 21321003) and Chinese Academy of Sciences. Dong-Pyo Kim acknowledges National Research Foundation of Korea (NRF) grant funded by the Korean Government (MEST) (No. 2008- 0061983). Also, we greatly appreciate Dr. Linlin Wang and Professor Dihua Shangguan from ICCAS for their kind help in flow cytometric quantification analysis and Dr. Xiaoge Wu from POSTECH for her fruitful discussion in fluorescent polymer nanothermometer application.

DOI: 10.1021/acs.analchem.5b02791
Anal. Chem. 2015, 87, 10535−10541

REFERENCES

(1) Warner, D. A.; Shine, R. *Nature* **2008**, *451*, 566−569.
(2) Huang, H.; Delikanli, S.; Zeng, H.; Ferkey, D. M.; Pralle, A. *Nat. Nanotechnol.* **2010**, *5*, 602−606.
(3) Xie, T.; McCann, U. D.; Kim, S.; Yuan, J.; Ricaurte, G. A. *J. Neurosci.* **2000**, *20*, 7838−7845.
(4) Dufour, S.; Rousse, N.; Canioni, P.; Diolez, P. *Biochem. J.* **1996**, *314*, 743−751.
(5) Brown, R.; Rickless, P. *Proc. R. Soc. London, Ser. B* **1949**, *136*, 110.
(6) Gota, C.; Okabe, K.; Funatsu, T.; Harada, Y.; Uchiyama, S. *J. Am. Chem. Soc.* **2009**, *131*, 2766−2767.
(7) Lowell, B. B.; Spiegelman, B. M. *Nature* **2000**, *404*, 652−660.
(8) Yang, J. M.; Yang, H.; Lin, L. W. *ACS Nano* **2011**, *5*, 5067−5071.
(9) Smith, G. D.; Gunthorpe, M. J.; Kelsell, R. E.; Hayes, P. D.; Reilly, P.; Facer, P.; Wright, J. E.; Jerman, J. C.; Walhin, J. P.; Ooi, L.; Egerton, J.; Charles, K. J.; Smart, D.; Randall, A. D.; Anand, P.; Davis, J. B. *Nature* **2002**, *418*, 186−190.
(10) Peng, H. S.; Stich, M. I. J.; Yu, J. B.; Sun, L. N.; Fischer, L. H.; Wolfbeis, O. S. *Adv. Mater.* **2010**, *22*, 716−719.
(11) Yu, J. B.; Sun, L. N.; Peng, H. S.; Stich, M. I. J. *J. Mater. Chem.* **2010**, *20*, 6975−6981.
(12) Sun, L. N.; Yu, J. B.; Peng, H. S.; Zhang, J. Z.; Shi, L. Y.; Wolfbeis, O. S. *J. Phys. Chem. C* **2010**, *114*, 12642−12648.
(13) Albers, A. E.; Chan, E. M.; McBride, P. M.; Ajo-Franklin, C. M.; Cohen, B. E.; Helms, B. A. *J. Am. Chem. Soc.* **2012**, *134*, 9565−9568.
(14) Tsuji, T.; Yoshida, S.; Yoshida, A.; Uchiyama, S. *Anal. Chem.* **2013**, *85*, 9815−9823.
(15) Okabe, K.; Inada, N.; Gota, C.; Harada, Y.; Funatsu, T.; Uchiyama, S. *Nat. Commun.* **2012**, *3*, 705.
(16) Uchiyama, S.; Kimura, K.; Gota, C.; Okabe, K.; Kawamoto, K.; Inada, N.; Yoshihara, T.; Tobita, S. *Chem.—Eur. J.* **2012**, *18*, 9552−9563.
(17) Kiyonaka, S.; Kajimoto, T.; Sakaguchi, R.; Shinmi, D.; Omatsu-Kanbe, M.; Matsuura, H.; Imamura, H.; Yoshizaki, T.; Hamachi, I.; Morii, T.; Mori, Y. *Nat. Methods* **2013**, *10*, 1232.
(18) Donner, J. S.; Thompson, S. A.; Kreuzer, M. P.; Baffou, G.; Quidant, R. *Nano Lett.* **2012**, *12*, 2107−2111.
(19) Ke, G. L.; Wang, C. M.; Ge, Y.; Zheng, N. F.; Zhu, Z.; Yang, C. J. *J. Am. Chem. Soc.* **2012**, *134*, 18908−18911.
(20) Shang, L.; Stockmar, F.; Azadfar, N.; Nienhaus, G. U. *Angew. Chem., Int. Ed.* **2013**, *52*, 11154−11157.
(21) Jaque, D.; Maestro, L. M.; Escudero, E.; Rodríguez, E. M.; Capobianco, J. A.; Vetrone, F.; Juarranz de la Fuente, A.; Sanz-Rodríguez, F.; Iglesias-delaCruz, M. C.; Jacinto, C.; Rocha, U.; García Solé, J. *J. Lumin.* **2013**, *133*, 249−253.
(22) Qiao, J.; Chen, C. F.; Qi, L.; Liu, M. R.; Dong, P.; Jiang, Q.; Yang, X. Z.; Mu, X. Y.; Mao, L. Q. *J. Mater. Chem. B* **2014**, *2*, 7544−7550.
(23) Ye, F. M.; Wu, C. F.; Jin, Y. H.; Chan, Y. H.; Zhang, X. J.; Chiu, D. T. *J. Am. Chem. Soc.* **2011**, *133*, 8146−8149.
(24) Qiao, J.; Mu, X. Y.; Qi, L. J. *J. Mater. Chem. B* **2013**, *1*, 5756−5761.
(25) Xie, J. P.; Zheng, Y. G.; Ying, J. Y. *J. Am. Chem. Soc.* **2009**, *131*, 888−889.
(26) Lai, J. T.; Filla, D.; Shea, R. *Macromolecules* **2002**, *35*, 6754−6756.
(27) Gúevel, X. L.; Daum, N.; Schneider, M. *Nanotechnology* **2011**, *22*, 275103.
(28) Aamer, K. A.; Tew, G. N. *J. Polym. Sci., Part A: Polym. Chem.* **2007**, *45*, 5618−5625.
(29) Hoang, P. H.; Nguyen, C. T.; Perumal, J.; Kim, D. P. *Lab Chip* **2011**, *11*, 329−335.
(30) Iwasaki, T.; Yoshida, J. *Macromolecules* **2005**, *38*, 1159−1163.
(31) Kawaguchi, T.; Miyata, H.; Ataka, K.; Mae, K.; Yoshida, J. *Angew. Chem., Int. Ed.* **2005**, *44*, 2413−2416.
(32) Yang, J.; Qi, L.; Chen, Y.; Ma, H. M. *Chin. J. Chem.* **2013**, *31*, 209−214.
(33) Al-Dirbashi, O.; Kuroda, N.; Nakashima, K. *Anal. Chim. Acta* **1998**, *365*, 169−176.
(34) Gibson, M. I.; O'Reilly, R. K. *Chem. Soc. Rev.* **2013**, *42*, 7204−7213.

DOI: 10.1021/acs.analchem.5b02791
Anal. Chem. 2015, 87, 10535−10541